Hadronic Scaling in the Scattering of Composite Systems*

Paul M. Fishbane
Physics Department,† University of Virginia, Charlottesville, Virginia 22901
and Institute for Theoretical Physics, State University of New York at Stony Brook, Stony Brook, New York 11790

J. S. Trefil
Physics Department, University of Virginia, Charlottesville, Virginia 22901
(Received 16 February 1973)

We discuss the problem of limiting behavior (scaling) in the inclusive scattering from composite systems when the inclusive scattering of their constituents is known to scale. In particular, the composite system we study is the nucleus, and the scattering formalism is a multiparticle form of the Glauber theory. The effects we study come from inelastic collisions of independent products of earlier inelastic collisions within a given nucleus, i.e., intranuclear cascading. At sufficiently high energies the distribution from nuclear scattering scales; the scaling function is very closely related to the scaling function for scattering from nucleons. The approach to scaling depends logarithmically on s but also on scattering properties of the constituent nucleons and on properties of the composite nucleus. When these factors are combined we are presented with a rather rich picture of the approach to the scaling limit. We present numerical calculations to illuminate this picture, and discuss possible experimental tests which can be performed with nuclear targets. We speculate on the application of our ideas to hadronic systems themselves and on the features of hadronic systems they may explain.

I. INTRODUCTION

Limiting behavior,[1] or Feynman scaling,[2] in hadron-hadron collisions states that at high energies cross sections for the inclusive process $a+b \to c+X$, where X is not detected, become functions only of the scaling variable $x = 2p_{\parallel}^{*c}/\sqrt{s}$, where $p_{\parallel}^{*c}$ is the longitudinal momentum of c in the center-of-mass system, and the transverse momentum $p_{\perp}^{c}$. Parton models[3] (or more generally the idea that the nucleon is composite) similarly, and not altogether independently, enjoy wide currency. Implicit in the idea of compositeness, however, is the fact that in collisions between composite systems multiple scattering between the constituents can and must occur. The problem of tying together limiting behavior with the necessary multiple scattering in hadron-hadron collisions has not been well understood.

In this paper, which is a detailed account of a summary of this work published elsewhere,[4] we examine the following problem: Suppose, in the inclusive scattering of composite systems, the scattering between the constituents of the systems is known to scale. What will be the scaling behavior, if any, of the inclusive scattering of the composite objects? In this paper we shall concentrate for concreteness on pionic scattering on nuclei,

$$\pi + A \to \pi + X,$$

where A is a nucleus composed of A constituent nucleons. We want to emphasize, however, that formulas and qualitative results which we find can be applied to the scattering of any composite system which has the characteristic that the binding energy is small compared to the scattering energy. Therefore we have in mind that our results and ideas may be ultimately applicable to hadronic systems themselves. The constituents of these systems might be regarded as "partons"; in fact, we often use the word parton to refer to the constituent component of whatever composite system we are considering. We reserve further discussion and speculation on hadronic processes until the conclusion of this paper.

The main dynamical effect which makes the nuclear cross section different from the nucleon cross section (aside from simply its greater mass and area) is the cascading of inelastic reactions which multiple scattering allows. This cascading, in which products of an initial inelastic collision undergo further inelastic collisions, can only take place if these products exist independently and incoherently within the nucleus. In particular, the detected species must be produced incoherently. This means that cascading cannot take place if the final-state particles are the decay products of a "coherent" hadronic excitation ("fireball") whose lifetime is long compared to a nucleon radius. One type of mechanism which might allow these final-state particles to come into immediate independent existence is a multiperipheral[5] type of reaction. We therefore assume throughout this paper that an incoherent type of production mechanism is domi-

nant above some fixed energy. If some type of coherent production mechanism (such as diffractive excitation[6]) were dominant, then our qualitative results would be quite different. Indeed nuclear-scattering distributions can help us to distinguish these two types of reactions, as we have discussed previously.[7,8]

We will show that in the case of reaction (1) the nuclear cross section will scale when the cross section for $\pi + N \to \pi + X$ scales. Furthermore, the scaling limit is a well-defined function of the parton-parton limiting cross section, and takes a form which is identical to the form one would expect if the partons scattered independently and incoherently. In this way our picture of limiting behavior is recursive, the scattering of composite systems approaching a scaling limit if the scattering of their constituents scales. Moreover, the approach to the scaling limit can be calculated, and depends on nuclear parameters and π-N scattering parameters as well as the energy; the main energy dependence is logarithmic. The pattern of this approach to scaling behavior is a complex one, as we shall see below.

The thrust of our approach is to use the nucleus as a "theoretical laboratory" to study the scaling behavior of weakly bound composite systems, for in this case we know the elementary interactions from other experiments and we know the nature and distribution of the constituent nucleons (a benefit we would not enjoy in treating a hadron composed of partons). In addition, we know that the Glauber theory[9] gives a good description of the multiple scattering of high-energy particles in nuclei at high energies. We do not believe that the results we find can depend on the particular multiple-scattering formalism we employ.

The plan of this paper is as follows: In Sec. II we present a review of the calculation of cascading in inelastic intranuclear events, using a multiparticle version[8,10] of the Glauber theory. This review includes discussion of the computation of all the different paths along which a cascade can develop. The problem divides naturally into two parts, given the distribution for $\pi + N \to \pi + X$: first, the problem of the distribution of the particles which are products of secondary inelastic collisions; and second, the probability of occurrence of these secondary collisions ("nuclear weight factors"). Both the secondary distributions and the nuclear weight factors depend on the multiplicity of the initial inelastic collision, i.e., on $\ln s$. In Sec. III, we separately examine the high-energy behavior of the distributions as well as the weight factors. This section is the heart of the paper and contains the discussion of the approach to the scaling limit. Section IV contains some numerical computations which are designed to confirm and elucidate the results of the previous section. Finally, Sec. V, which is divided into two parts, is concerned with tests and applications of our results to nuclear-scattering experiments, and with speculative remarks on the relevance of these results to improvement of our understanding of hadronic phenomena.

II. REVIEW OF THE INTRANUCLEAR CASCADE THEORY

A. Diagrams and Distributions

In a previous work,[8] the theory of the intranuclear cascade was worked out in some detail. In this section, we present a review of that theory, emphasizing the points which we will need in our discussion of scaling later in the paper.

We assume that particles belonging to the final state of an hadronic reaction which can participate in an intranuclear cascade process are not the end products of an hadronic excitation which lives longer than the radius of the nucleon (such as a "fireball"[6]). In other words, particles which participate in such a cascade must be independently and incoherently created within the nucleus. To this extent we shall be referring throughout this paper to incoherent production processes (IPP) rather than coherent production processes (CPP) as the primary collision mechanism. (We have previously[7,8] discussed how nuclear-scattering experiments can help distinguish between these two primary collision mechanisms. Multiple scattering when CPP dominate has its own distinctive signature.[11])

The reaction $\pi + N \to \pi + X$ can cascade in many possible ways in the nucleus to contribute to the process $\pi + A \to \pi + X$. The diagram in Fig. 1 is one such way. In this diagram, the incident particle penetrates into the nucleus to the point z_1, where an inelastic collision takes place. Let ϕ represent the number of particles created in this collision. Then each of these ϕ particles will proceed through the nucleus, and some of them will undergo inelastic collisions themselves (for example, at z_2, z_3, and z_4 in Fig. 1), creating still more particles. Between inelastic collisions, each particle can undergo[12] any number of elastic scatterings from nucleons. It is clear that, if we wish to calculate the rapidity distribution of outcoming particles, we must perform a properly weighted sum over the distribution for any diagram which leads to particles of the type we wish to measure coming out of the nucleus. The problem of calculation, then, falls naturally into three pieces: (i) computing the rapidity distribution for any given diagram, (ii) counting the diagrams,

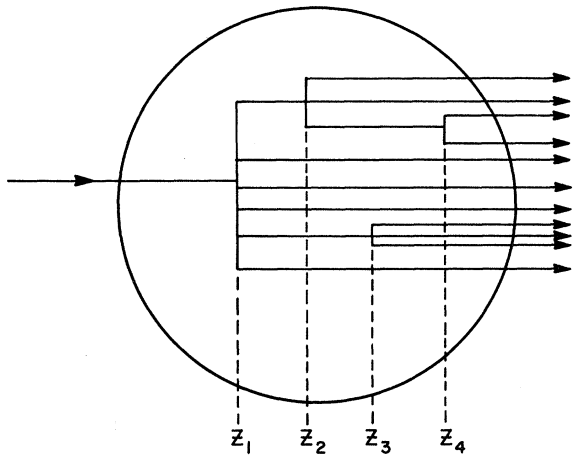

FIG. 1. Example of a possible intranuclear cascade. An initial inelastic collision takes place at z_1, with subsequent inelastic collisions at z_2, z_3, and z_4. Before, after, and in between inelastic collisions the particles undergo any number of elastic collisions.

and (iii) determining the appropriate weight for each diagram. In principle the "nuclear physics," i.e., how we perform the multiple-scattering calculation in a given nucleus, affects both (i) and (iii). However, when elastic and total cross sections are taken constant, category (i) becomes a property only of the topology of the given diagram, so that the nuclear effects appear only in (iii).

Let the rapidity distribution of final pions from the reaction $\pi + N \to \pi + X$ be given by

$$\left(\frac{dn}{dr}\right)_1 = h_1(r_{\max}, r), \tag{2.1}$$

where $r_{\max}$ is the maximum rapidity which the measured outcoming pion can have consistent with energy conservation, and r is the rapidity which it actually does have. In the case where both the incoming and outgoing particles are pions, $r_{\max}$ is the rapidity of the incident particle as well. (In what follows, we will consider this case only.) As our notation implies, we have normalized this distribution in the usual manner, so that the mean number of produced pions is

$$\phi = \int_0^{r_{\max}} dr\, h_1(r_{\max}, r). \tag{2.2}$$

It is not necessary at this point to assume that our primary distribution scales; we shall make this explicit assumption when it becomes necessary.

Let us label the "generation" of a pion by the number of inelastic collisions which separate it from the incoming projectile. Thus, in Fig. 1, pions proceeding from z_1 are first-generation, those from z_2 or z_3 are second-generation, etc.

Consider now the second generation. A second-generation pion originating in a given inelastic collision would have a rapidity distribution given by $h_1(r_1, r_2)$, where r_1 is the rapidity of the first-generation pion causing this inelastic collision. To get the actual distribution of second-generation pions, we would have to multiply this by the probability of producing a pion of rapidity r_1 in the first generation, and then add up over all r_1. Thus we have

$$h_2(\phi; r_{\max}, r_2) = \frac{\int_{r_2}^{r_{\max}} h_1(r_{\max}, r_1) h_1(r_1, r_2) dr_1}{\int_0^{r_{\max}} h_1(r_{\max}, r_1) dr_1} \tag{2.3}$$

for the distribution of a second-generation pion. Note that we have included explicit ϕ dependence to show that h_2 will not scale in general; this is true even though h_1 is taken to scale at low energies. The mean number of pions produced in a second-generation collision is then

$$\phi_2 = \int_0^{r_{\max}} h_2(\phi; r_{\max}, r_2) dr_2 . \tag{2.4}$$

Similarly the distribution for an nth-generation pion will be

$$h_n(\phi; r_{\max}, r_n) = \frac{\int h_1(r_{\max}, r_1) h_1(r_1, r_2) \cdots h_1(r_{n-1}, r_n) dr_1 \cdots dr_{n-1}}{\phi_{n-1}\phi_{n-2}\cdots\phi_1} = \frac{\int h_{n-1}(\phi; r_{\max}, r_{n-1}) h_1(r_{n-1}, r_n) dr_{n-1}}{\phi_{n-1}}, \tag{2.5}$$

with a corresponding mean multiplicity ϕ_n given by

$$\phi_n = \int_0^{r_{\max}} dr\, h_n(\phi; r_{\max}, r). \tag{2.6}$$

With these distributions and the assumption of energy-independent cross sections (so that elastic scattering in the nucleus does not affect the rapidity distribution of final pions for the given diagram), we can then in principle write the rapidity distribution for any diagram simply by counting the number of pions coming from a given generation. This count of course depends on more than the average number of pions produced in an inelastic collision. In principle there are two types of effects we must include if we wish to compute the rapidity distribution for any diagram. (i) There is dispersion in the number of particles produced in each inelastic collision. (For a fixed energy, the number of pions produced in the initial collision obviously affects the probability of a second inelastic collision.) (ii) Each particle in the $(n-1)$th generation will have a different energy and therefore on energy grounds alone will give rise to different numbers of produced pions should

it happen to initiate the nth generation.

At this point we make two (related) simplifying assumptions. We assume that the number of pions produced in any inelastic collision is exactly the mean for that class of collisions. (At large ϕ this is expected to be satisfactory.) We similarly assume that every pion in the $(n-1)$th generation initiating an nth-generation event produces exactly ϕ_n pions. For example, the initial collision produces exactly ϕ pions, *every* second-generation collision produces ϕ_2 pions, etc. This type of assumption is standard when one wishes to deal only with average properties of a cascade, and, in particular, is adequate for the single-particle distribution we are attempting to compute.

If we make these assumptions, it becomes simple to compute the rapidity distribution for any diagram. For example, the net distribution from the diagram in Fig. 1 is just

$$\left(\frac{dn}{dr}\right)_{\text{Fig. 1}} = \frac{\phi-2}{\phi}h_1 + \frac{2\phi_2-1}{\phi_2}h_2 + \frac{\phi_3}{\phi_3}h_3 . \quad (2.7)$$

To complete the discussion of diagrams, we now note that under our averaging and constant cross-section assumptions, there are many different diagrams which would give exactly this distribution. For example, if the second generation at z_2 were caused by the second pion from the top, rather than the first, the result of Eq. (2.7) would be exactly the same. We will label all graphs which give identical (dn/dr) as a "sequence," and the distribution summed over all of the graphs in a sequence as $\langle dn/dr\rangle_s$. Clearly, $\langle dn/dr\rangle_s$ will just be (dn/dr) times the number of diagrams in a given sequence. This is an easy number to calculate for each sequence. For example, in Fig. 1, there are $\binom{\phi}{2}$ ways of picking the two pions which will cause second-generation events, and $\binom{2\phi_2}{1}$ ways of picking the pion which will cause a third generation. Thus

$$\left\langle\frac{dn}{dr}\right\rangle_{\text{Fig. 1}} = \binom{\phi}{2}\binom{2\phi_2}{1}\left(\frac{dn}{dr}\right)_{\text{Fig. 1}} \equiv a(\phi, N)\left(\frac{dn}{dr}\right)_{\text{Fig. 1}} . \quad (2.8)$$

The final distribution is the sum of the distributions for all possible sequences, weighted by nuclear effects. It is convenient to determine sequences by first fixing N, the number of inelastic collisions. For $N=1$, there is only the one sequence. For $N=2$, there is also only one sequence, with distribution

$$\left\langle\frac{dn}{dr}\right\rangle_{N=2} = \binom{\phi}{1}\left(\frac{\phi-1}{\phi}h_1 + h_2\right), \quad (2.9)$$

and so forth.

B. Nuclear Weight Factors

The probability of any particular sequence of course depends on the properties of the nucleus. We use the Glauber theory,[9] as developed for a sequential series of inelastic collisions,[13] to describe the effects of the nucleus. The contribution to the doubly differential nuclear cross section for a given sequence α involving N inelastic collisions is just[8]

$$\left(\frac{d\sigma}{dr\,d\Delta^2}\right)_\alpha = \sigma_{\text{in}}^T \left\langle\frac{dn}{dr}\right\rangle_\alpha \frac{1}{4\pi}\binom{A}{N}\int e^{i\vec{\Delta}\cdot(\vec{b}-\vec{b}')} d^2b\, d^2b' \prod_{i=1}^{A}\rho(\vec{s}_i, z_i)d^2s_i\, dz_i \times \prod_{j=1}^{N}\Gamma_{\text{in}}(\vec{b}-\vec{s}_j)\Gamma_{\text{in}}^*(\vec{b}'-\vec{s}_j) \prod_{z_a<z_1}\{[1-\Gamma_{\text{el}}(\vec{b}-\vec{s}_a)][1-\Gamma_{\text{el}}^*(\vec{b}'-\vec{s}_a)]\}^1 \times \prod_{z_1<z_b<z_2}\{[1-\Gamma_{\text{el}}(\vec{b}-\vec{s}_b)][1-\Gamma_{\text{el}}^*(\vec{b}'-\vec{s}_b)]\}^{n_1}\times\cdots , \quad (2.10)$$

where A is the number of nucleons, $\vec{\Delta}$ the transverse momentum transfer to the nucleus, r the rapidity of the single measured outcoming pion, $\rho(\vec{s}_i, z_i)$ the ground-state density of the ith nucleon whose coordinate is $\vec{r}_i = (\vec{s}_i, z_i)$, and $\vec{b}$ and $\vec{b}'$ impact parameters. Note that the rapidity-dependent term $\langle dn/dr\rangle_\alpha$ factors out of all integrations. The transverse-momentum distributions of inelastic collisions are contained, as we state more explicitly below, in the inelastic profile functions. We have written Eq. (2.10) in the form of a cross section; this can be converted to a number distribution by division by the total inelastic cross section σ_{in}^T, in the usual fashion.[1]

The profile functions Γ are related to pion-nucleon scattering amplitudes by

$$\Gamma_c(\vec{b}) = \frac{1}{2\pi p}\int e^{-i\vec{q}\cdot\vec{b}} f_c(q)d^2q ,$$

where

$$f_c(q) = ipQ_c\, e^{-a_c q^2/2}$$

and where c is either "in" or "el," depending on whether we are discussing inelastic or elastic scattering. In the former case $Q_{\text{in}} = (\sigma_{\text{in}} a_{\text{in}}/\pi)^{1/2}$, while in the latter $Q_{\text{el}} = (1/4\pi)\sigma_T$, where σ_{in} and σ_T are the inelastic and the total pion-nucleon cross section, respectively, and a_{in} is the width of the

inclusive inelastic peak.

Equation (2.10) admits of a particularly simple interpretation. The term

$$\prod_{z<z_1}[(1-\Gamma)(1-\Gamma^*)]^1$$

describes the propagation of the incident particle up to z_1, allowing it to scatter elastically any number of times on nucleons to the left of z_1. This takes into account the "absorption" of the incoming particle.[12] The term $\Gamma_{\text{in}}(\vec{b}-\vec{s}_1)\Gamma^*_{\text{in}}(\vec{b}'-\vec{s}_1)$ represent the inelastic scattering at z_1. The term

$$\prod_{z_1<z<z_2}[(1-\Gamma)(1-\Gamma^*)]^{n_1}$$

represents the propagation of n_1 particles from z_1 to z_2 by elastic scattering. In Fig. 1, for example, n_1 would be 6. The rest of the terms in Eq. (2.10) can be similarly interpreted.

Equation (2.10) represents the basic working equation for describing the nuclear physics, so we will review here several features of the Glauber theory[9] which are already incorporated into it: (i) The final state of the nucleus has been summed over by using closure, so that no restriction is made on what happens to the nucleus after the collision. (ii) When many pions are propagating across the nucleus, each pion can scatter elastically only once off of any nucleon. Thus, while each nucleon may serve as an elastic-scattering target for any number of pions in succession, it may not be struck twice by any given pion. (iii) All scattering is on-shell. (iv) The nucleons on which inelastic collisions occur are treated quite differently from the nucleons off which elastic scattering occurs. These N nucleons are allowed to serve as targets for only one interaction. The physical reasoning behind this assumption is that in an inelastic reaction, the nucleon is unlikely to retain its identity after the collision. Thus, a pion arriving at the site of the nucleon in the wake of an inelastic collision would find there the fragments of the target nucleon, e.g., pions, $\bar{N}N^*$ pairs, other mesons, and, perhaps, a recoiling nucleon. The interaction of the pion with this debris is neglected, just as the interaction between pions created in different inelastic collisions is neglected. We regard this as neglecting the effect of final-state interactions between products of different inelastic collisions (although the final-state interactions between particles created in the same collision are presumably included in the form of the primary distribution h_1.)

Assumption (iv) has the effect of limiting the number of possible inelastic scatterings to A, the nucleon number. While this is not of great importance for the discussion of cosmic-ray or accelerator data, since we find adequate numerical convergence for some value of N less than A, it will be crucial to our discussion of scaling in the next section. For this reason, we regard the question of whether this assumption can be relaxed to be of the greatest interest. We also note however that if the number of allowed inelastic reactions were simply fixed at some value other than A, then our qualitative results would be unchanged.

The approximations (i), (ii), and (iii) discussed above are inherent in the Glauber theory. In order to carry out the integrals over the nuclear coordinates easily, we found it necessary to make another approximation,[13] which we call the "rim approximation." In this approximation, all pions which do not subsequently suffer inelastic collisions are assumed to commence elastic scattering at the plane $z=0$, rather than at $z_1, z_2, \ldots$. As we discussed previously,[8] we do not expect this to be a bad approximation since the inelastic collisions will be taking place in both halves of the nucleus. It must be emphasized, however, that no such approximation is made for the inelastic collisions, so that all positions of z_2, for example, are summed over.

Let us take for the ground-state nucleon density functions in a given nucleus:

$$\rho(\vec{s},z)=\rho_0\exp\left(-\frac{\vec{s}^{\,2}+z^2}{R^2}\right).$$

We can then simplify the integral over $\vec{\Delta}$ of Eq. (2.10) by the successive substitutions $\vec{B}=\frac{1}{2}(\vec{b}+\vec{b}')$ and $y=\exp(-B^2/R^2)$. We find

$$\left(\frac{d\sigma}{dr}\right)_\alpha=\int d\Delta^2\left(\frac{d\sigma}{dr\,d\Delta^2}\right)_\alpha$$
$$=\sigma_{\text{in}}^T\left\langle\frac{dn}{dr}\right\rangle_\alpha\binom{A}{N}\left(\frac{\sigma_{\text{in}}}{\pi R^2}\right)^N\left(\frac{R^2}{a_{\text{in}}+R^2}\right)^N R^2$$
$$\times\int_0^1 dy\,y^{NR^2/(a_{\text{in}}+R^2)-1}\left[\sum_{k=0}^{2}\binom{2}{k}\gamma^k\frac{2a_{\text{el}}}{2a_{\text{el}}+kR^2}\,y^{kR^2/(kR^2+2a_{\text{el}})}\right]^{(A-N)/2}$$
$$\times\left[\sum_{k=0}^{2n}\binom{2n}{k}\gamma^k\frac{2a_{\text{el}}}{2a_{\text{el}}+kR^2}\,y^{kR^2/(kR^2+2a_{\text{el}})}\right]^{(A-N)/2} \tag{2.11}$$
$$\equiv\sigma_{\text{in}}^T\left\langle\frac{dn}{dr}\right\rangle_\alpha\sigma_N^n. \tag{2.12}$$

In this equation $\gamma = -\sigma_T/(4\pi a_{el})$, and n is the total number of pions which emerge from the nucleus. Under our assumption of no dispersion in the number distribution for inelastic collisions, n is a straightforward function of ϕ and the particular sequence. The sums over k represent the propagation of particles through the nucleus by elastic scattering.

We see that the nuclear effects are completely included in the term σ_N^n, which we must now evaluate if we are to proceed farther. Before we evaluate these factors, let us complete the formal development. The cross section is found by summing Eq. (2.12) over sequences α:

$$\begin{aligned}\frac{d\sigma}{dr} &= \sum_\alpha \left(\frac{d\sigma}{dr}\right)_\alpha \\ &= \sigma_{\text{in}}^T \sum_\alpha \left\langle \frac{dn}{dr} \right\rangle_\alpha \sigma_N^n \\ &= \sigma_{\text{in}}^T \sum_\alpha \left(\frac{dn}{dr}\right)_\alpha a(\phi, N)\sigma_N^n . \end{aligned} \tag{2.13}$$

Since $(dn/dr)_\alpha$ is already in the form of a number distribution, we find the number distribution for the process $\pi + A \to \pi + X$ to be

$$\left.\frac{dn}{dr}\right|_A = \frac{\sum_\alpha (dn/dr)_\alpha a(\phi, N)\sigma_N^n}{\sum_\alpha a(\phi, N)\sigma_N^n} . \tag{2.14}$$

This distribution is of course normalized so that, when $dn/dr|_A$ is integrated over r, it yields the average number of pions produced in the nuclear collision.

C. Evaluation of the Nuclear Weight Factors for Large Energies

Although Eq. (2.11) is already in a form which is suitable for computer evaluation (see Sec. IV), a great deal of insight can be gained by analytic evaluation of these nuclear processes at high energies. In this section, we shall concern ourselves with the evaluation of the nuclear weight factors σ_N^n, and will discuss the other factors in Eq. (2.11) in a later section.

The chief difficulty in writing a simple expression for the nuclear weights are the sums which appear raised to the $(A - N)/2$ power in Eq. (2.11). We shall evaluate these sums by expanding in the parameter a_{el}/R^2. We shall assume that this parameter is small (indeed, it is less than 0.1 for typical nuclei), so that only a few terms in the expansion need be kept.

The physical meaning of this approximation in the case of a nucleus is quite simple. Since a_{el}, which determines the width of the pion-nucleon diffraction peak, is roughly the size of the proton, a_{el}/R^2 is simply the ratio of the size of the nucleon to the size of the nucleus. If one has some other application in mind, where $a_{el} \approx R^2$ (say, in parton-type models of hadron-hadron scattering), then it is straightforward to include higher-order terms.

In this case, we can write

$$\begin{aligned}\mathcal{S} &\equiv \sum_k \binom{2n}{k} \gamma^k \frac{2a_{el}}{2a_{el} + kR^2} y^{kR^2/(2a_{el}+kR^2)} \\ &= 1 + \frac{2a_{el}}{R^2} y S_1 - \left(\frac{2a_{el}}{R^2}\right)^2 y(1 + \ln y) S_2 + \cdots , \end{aligned} \tag{2.15}$$

where we have set

$$S_m = \sum_{k=1}^{2n} \binom{2n}{k} \frac{\gamma^k}{k^m} . \tag{2.16}$$

The sums S_m, which involve alternating series of large terms, are difficult to evaluate as they stand, but in the Appendix they are shown to have a simple value for large n, which is just

$$\lim_{n\to\infty} S_m = -\frac{1}{m!} \ln^m(2n) . \tag{2.17}$$

Although the series therefore formally diverges in the limit $n \to \infty$, the ratio of successive terms only grow as $\ln n \sim \ln \ln s$, and the first term S_1 numerically dominates when

$$\frac{2a_{el}}{R^2} \ln n \ll 1 . \tag{2.18}$$

This inequality will be satisfied for typical values of a_{el} and R^2 provided that $n \ll 10^6$, which is certainly true in any case of physical interest. Thus we have

$$\mathcal{S} \approx 1 - \frac{2a_{el}}{R^2} y \ln n . \tag{2.19}$$

By Eq. (2.18) we may make the approximation

$$(1 - \epsilon)^Q \underset{\epsilon \to 0}{\approx} e^{-\epsilon Q} ,$$

so that

$$\mathcal{S}^{(A-N)/2} \approx \exp\left[-y \frac{a_{el}}{R^2} (A - N) \ln n \right] . \tag{2.20}$$

The other summation $\mathcal{S}'$ raised to the $(A - N)/2$ power in Eq. (2.11) can be dealt with in a similar way. The summation is connected formally with the propagation of the incident particle in the nucleus, and hence does not depend on n. We can still keep lowest-order terms in a_{el}/R^2, however, to write

$$\begin{aligned}(\mathcal{S}')^{(A-N)/2} &= \left[\sum_{k=1}^{2} \binom{2}{k} \gamma^k \frac{2a_{el}}{2a_{el} + kR^2} y^{2a_{el}/(kR^2 + 2a_{el})} \right]^{(A-N)/2} \\ &\approx \exp\left[y \frac{(A - N)a_{el}}{R^2} \sum_{k=1}^{2} \binom{2}{k} \frac{\gamma^k}{k} \right] . \end{aligned} \tag{2.21}$$

Since γ is a number less than 1, and $\ln n$ is presumably large compared to 1 at high energies [although not so large that Eq. (2.18) is violated], we can write

$$(\mathcal{S}\mathcal{S}')^{(A-N)/2} \approx \mathcal{S}^{(A-N)/2} . \tag{2.22}$$

Since we expect that the target areas which determine the width of the diffraction peak in the inclusive reaction (a_{in}) and in elastic scattering (a_{el}) will both be much less than R^2, it is consistent with the above approximations to write

$$y^{NR^2/(a_{\text{in}}+R^2)} \approx y^N .$$

Putting these results together, we have

$$\sigma_N^n = \binom{A}{N}\left(\frac{\sigma_{\text{in}}}{\pi R^2}\right)^N R^2 \int_0^1 dy\, y^{N-1} e^{-\alpha y} , \tag{2.23}$$

where we have written

$$\alpha \equiv (A-N)\frac{a_{\text{el}}}{R^2}\ln n . \tag{2.24}$$

Then

$$\sigma_N^n = R^2\binom{A}{N}\left(\frac{\sigma_{\text{in}}}{\pi R^2}\right)^N \frac{\gamma(N,\alpha)}{\alpha^N} , \tag{2.25}$$

where $\gamma(N,\alpha)$ is the incomplete γ function.

We shall consider two separate limits of this function, depending on the value of the parameter α. This parameter will play an important role in our scaling argument, and will ultimately determine the approach to scaling behavior of each nucleus. We have

$$\sigma_N^n \approx R^2\binom{A}{N}\left(\frac{\sigma_{\text{in}}}{\pi R^2}\right)^N \frac{(N-1)!}{\alpha^N} \tag{2.26}$$

for α large, and

$$\sigma_N^n \approx R^2\binom{A}{N}\left(\frac{\sigma_{\text{in}}}{\pi R^2}\right)^N \frac{1}{N} \tag{2.27}$$

for α small.

III. THE SCALING LIMIT

We have now discussed the weights of a given sequence, the counting of sequences, and the rapidity (or x) distribution $h_i(\phi; r_{\max}, r)$ of ith-generation pions, and how the different factors are combined to give the rapidity distribution for inclusive scattering on a nucleus. We have seen that all these factors depend on the incoming energy through the primary collision multiplicity ϕ. The question of what happens at very large energies is then most simply answered by investigating separately the behavior of the h_i and their coefficients (these coefficients having been determined by the nuclear weights and the counting factors). We shall see that at large energy both the coefficients and the h_i approach scaling behavior, so that the nuclear scattering process scales. The h_i approach scaling limits when $\phi \gg 1$. The nuclear weight coefficients approach their limits in a much more complicated way, and for typical problems they require larger energies to reach their limit than the energies required for the h_i to scale.

The plan of this section, then, is as follows: In Sec. III A we discuss the approach to the scaling limits of the distributions $h_i(\phi; r_{\max}, r)$. In Sec. III B we discuss the behavior of the coefficients by example. Finally, in Sec. III C, we put these results together to find the scaling behavior of the nuclear distribution.

A. Limiting Behavior of the h_i

The secondary collision distributions $h_i(\phi; r_{\max}, r)$ defined in Eq. (2.5) do not scale for arbitrary $r_{\max}$ even though the primary distribution h_i may do so. An illustration of this nonscaling behavior can be seen explicitly in the example worked out at the end of this section, where $h_n(\phi; r_{\max}, r)$ depends on the ratio $r/r_{\max}$ rather than on the variable x. Nevertheless, in the limit of large $r_{\max}$, we shall show that the h_i approach a scaling limit. In particular, in the projectile fragmentation region all of the h_i except h_1 go to zero, while in the target fragmentation region all of the h_i become equal to h_1.

In order to show this, we separate the primary distribution $h_1(r_{\max}, r)$ into fragmentation and pionization regions, marked off arbitrarily well by a cutoff rapidity r_c:

$$h_1(r_{\max}, r) = f(r)\theta(r)\theta(r_c - r) + a\theta(r - r_c)\theta(r_{\max} - r_c - r) + \tilde{f}(r_{\max} - r)\theta(r - r_{\max} + r_c)\theta(r_{\max} - r) , \tag{3.1}$$

for $r_{\max} > 2r_c$. The three terms represent respectively the target fragmentation, pionization, and projectile fragmentation regions. If $r_{\max} < 2r_c$, then we could write an analogous two-term form; we shall not concern ourselves with this case.

Consider now Eq. (2.3) defining $h_2(\phi; r_{\max}, r)$. The denominator takes the form

$$\begin{aligned} D &\equiv \int_0^{r_{\max}} h_1(r_{\max}, r)\,dr \\ &= \int_0^{r_c} f(r)\,dr + a\int_{r_c}^{r_{\max}-r_c} dr + \int_{r_{\max}-r_c}^{r_{\max}} \tilde{f}(r_{\max} - r)\,dr \\ &= a r_{\max} + \text{finite terms} . \end{aligned} \tag{3.2}$$

Next consider the numerator,

$$N \equiv \int_r^{r_{\max}} h_1(r_{\max}, r')h_1(r', r)\,dr' .$$

We shall study the following three regions for r.

(a) $r < r_c$ (target fragmentation). Break the integral up into two terms:

$$N=\int_{r}^{2r} dr'[f(r')\theta(r_c-r')+a\theta(r'-r_c)]\tilde{f}(r'-r)$$
$$+\int_{2r}^{r_{\max}} dr'[f(r')\theta(r_c-r')+a\theta(r_c-r')\theta(-r'+r_{\max}-r_c)+\tilde{f}(r_{\max}-r')\theta(r'-r_{\max}+r_c)]$$
$$\times[f(r)+\tilde{f}(r'-r)\theta(r-r'+r_c)].$$

To proceed further it is convenient to study the two cases $2r \leq r_c$ and $2r \geq r_c \geq r$ separately. In each case it is straightforward to show that the region where one $f(r')$ term overlaps the pionization term of the other factor is dominant, giving

$$N=f(r)ar_{\max}+\text{finite terms}.$$

Combining this with our result for D, Eq. (3.2),

$$h_2(\phi; r_{\max}, r)=f(r)+O(\phi^{-1}) \tag{3.3}$$

in the target fragmentation region. It is straightforward to generalize this result in higher orders:

$$h_i(\phi; r_{\max}, r)=f(r)+O(\phi^{-1}), \tag{3.4}$$

i.e., a result which scales and is just the same as h_1 in this region.

(b) $r > r_{\max}-r_c$ (projectile fragmentation). In this case the integration range of N is of width $\leq r_c$. This finite range gives a finite result, which, combined with the growing result for D, implies

$$h_2(\phi; r_{\max}, r)=O(\phi^{-1}) \tag{3.3'}$$

in the projectile-fragmentation region. This result similarly generalizes for all i,

$$h_i(\phi; r_{\max}, r)=O(\phi^{-1}). \tag{3.4'}$$

(c) $r_c < r < r_{\max}-r_c$ (pionization). The integration range of N is now a finite fraction β of $r_{\max}$, so that we get contributions from overlaps of both f and $\tilde{f}$ with pionization regions. Thus h_i tends to a finite limit which depends on the fractional length β as well as the details of both fragmentation regions of h_1.

In order to illustrate these general results consider an elementary distribution of the form

$$h_1(r_m, r)=\begin{cases}1, & r<r_m\\ 0, & r>r_m.\end{cases} \tag{3.5}$$

Some simple integrations then yield

$$h_n=[1-(r/r_m)]^{n-1}. \tag{3.6}$$

To show scaling in general, it is necessary to show that the h_i become functions of the variable x only. In general,

$$r=\tfrac{1}{2}r_m+\ln[x^{\frac{1}{2}}e^{r_m/2}+(x^2\tfrac{1}{4}e^{r_m}+1)^{1/2}], \tag{3.7}$$

so that

$$1-\frac{r}{r_m}=\frac{1}{2}-\frac{1}{r_m}\ln[x^{\frac{1}{2}}e^{r_m/2}+(x^2\tfrac{1}{4}e^{r_m}+1)^{1/2}].$$

If we confine our attention to the case $x^2\tfrac{1}{4}e^{r_m} \gg 1$ (i.e., look at nonwee x only), then

$$1-\frac{r}{r_m}=\frac{1}{2}-\frac{1}{r_m}\ln\left[(x+|x|)^{\frac{1}{2}}e^{r_m/2}+\frac{|x|}{x^2}e^{-r_m/2}\right]. \tag{3.8}$$

For x negative (target-fragmentation region), $x+|x|=0$, so that

$$1-\frac{r}{r_m}=1+\frac{\ln|x|}{r_m} \tag{3.9}$$

and

$$h_n(r_m, r) \underset{r_m\to\infty}{\sim} 1+O\left(\frac{(n-1)\ln|x|}{r_m}\right). \tag{3.10}$$

On the other hand, for $x>0$ (projectile-fragmentation region),

$$1-\frac{r}{r_m}=-\frac{1}{r_m}\ln x, \tag{3.9'}$$

so

$$h_n(r_m, r) \underset{r_m\to\infty}{\sim} 0+O((\ln x/r_m)^{n-1}). \tag{3.10'}$$

If we look at the pionization region, $x^2\tfrac{1}{4}e^{r_m} \ll 1$, we find

$$1-\frac{r}{r_m}=\frac{1}{2}-\frac{1}{r_m}\tfrac{1}{2}xe^{r_m/2}, \tag{3.9''}$$

so that

$$h_n(r_m, r) \underset{r_m\to\infty}{\sim} (\tfrac{1}{2})^{n-1}+O(\tfrac{1}{2}(n-1)xe^{r_m/2}/r_m). \tag{3.10''}$$

From this simple example, then, we confirm that (i) the secondary distributions h_i approach a definite limit at large energies; (ii) in the fragmentation regions, limiting forms of the h_i can be expressed simply in terms of h_1, the elementary distribution, while in the pionization region, the limiting form depends on h_1 in a more complicated way; and, finally, (iii) the approach to scaling is different in all three regions, and depends explicitly on the value of x, although the x dependence is only logarithmic.

B. Limiting Behavior of the Nuclear Coefficients

The general form of dn/dr for a reaction on a nucleus was presented in Eq. (2.14). The terms of

that equation take on a particularly simple form if we assume that

$$\phi \gg A . \tag{3.11}$$

In this regime, which corresponds to a different energy for each nucleus, the coefficients of the h_i in the expression for $(dn/dr)_\alpha$ [i.e., the distribution for a given graph, without the counting factor $a(\phi, N)$] become non-negative integers c_i^α independent of ϕ,

$$\left(\frac{dn}{dr}\right)_\alpha = \sum_{i=1}^{N} c_i^\alpha h_i . \tag{3.12}$$

The c_i^α have the following two special properties:

$$\sum_{i=1}^{N} c_i^\alpha = N , \tag{3.13}$$

and

$$c_1^\alpha = 1 . \tag{3.14}$$

Equation (3.13) follows because when there are N inelastic collisions and $\phi \gg N$, then N distribution functions h_i must appear, while Eq. (3.14) follows from the fact that there is but one primary collision.

As an example, in this limit Eq. (2.7) becomes

$$\left(\frac{dn}{dr}\right)_{\text{Fig. 1}} = h_1 + 2h_2 + h_3 . \tag{3.15}$$

In this example we only required that ϕ be large compared to one. In a graph in which the ϕ first-generation pions undergo A inelastic collisions we would require $\phi \gg A$ to approximate $(\phi - A)/\phi \approx 1$.

In addition, the graph counting factor $a(\phi, N)$, which is in general a rather complicated expression, becomes

$$a(\phi, N) \underset{\phi \gg A}{\sim} \phi^{N-1} b_\alpha , \tag{3.16}$$

where b_α is a positive number less than one which depends on the particular sequence α. For example, the counting factor for the sequence in Fig. 1 [see Eq. (2.8)] is just

$$a(\phi, N)\big|_{\text{Fig. 1}} = \phi(\phi - 1)\phi_2 = b_{\text{Fig. 1}}\, \phi^3 , \tag{3.17}$$

which for the simple distribution of Eq. (3.5) yields

$$b_{\text{Fig. 1}} = \tfrac{1}{2} .$$

There are precisely 2^{N-2} sequences to be considered for the terms with N inelastic collisions. The b_α have the property that for just those terms with N inelastic collisions

$$\sum_{\alpha=1}^{2^{N-2}} b_\alpha = O(1) . \tag{3.18}$$

Finally, we note that the nuclear factor depends on n, the number of particles emerging from the nucleus, through the incomplete γ function in Eq. (2.25). Since the parameter α depends on n only logarithmically, and since for any sequence $n = a\phi$, where [with the approximation of Eq. (3.11)] $a \ll \phi$, we can write

$$\sigma_N^n \approx \sigma_N^\phi . \tag{3.19}$$

For example, for Fig. 1,

$$n = \phi - 2 + 2\phi_2 - 1 + \phi_3 \approx \phi + 2\phi_2 + \phi_3 , \tag{3.20}$$

which for the distribution of Eq. (3.5) gives $a = 1 + \frac{2}{2} + \frac{1}{3} = \frac{7}{3}$.

With the approximations of Eqs. (3.12) and (3.19), which follow from the assumption that ϕ is large compared to A, the expression in Eq. (2.14) becomes

$$\left.\frac{dn}{dr}\right|_A^{N_{\max}} = \frac{\sigma_1^\phi h_1 + \phi\sigma_2^\phi(h_1 + h_2) + \cdots + \phi^{N_{\max}-1}\sigma_{N_{\max}}^\phi \sum_{\alpha=1}^{2^{N_{\max}-2}} b_\alpha \left(\sum_{i=1}^{N_{\max}} c_i^\alpha h_i\right)}{\sigma_1^\phi + \phi\sigma_2^\phi + \cdots + \phi^{N_{\max}-1}\sigma_{N_{\max}}^\phi \sum_{\alpha=1}^{2^{N_{\max}-2}} b_\alpha} . \tag{3.21}$$

In this equation, we have carried out the sum over inelastic scatterings to $N_{\max}$. The question of how many inelastic scatterings are to be allowed in a nucleus is, as we have pointed in Sec. II, crucial to our derivation. In all that follows, we shall use the arguments given above to set

$$N_{\max} = A . \tag{3.22}$$

However, it must be stressed that all of the significant features of our results would be the same if we chose some other $N_{\max}$ provided that $N_{\max}$ depended only on the nucleus and not on the energy.

It is also useful to rearrange the terms in the above equation and define new quantities $\mathcal{C}_i$ by writing

$$\frac{dn}{dr} = \sum_{i=1}^{A} \mathcal{C}_i h_i . \tag{3.23}$$

It may be worthwhile to pause at this point to consider the case $\phi \lesssim A$, which we have explicitly excluded in the above derivation. This case presents numerical difficulties in calculating the approach to scaling. (It is clear that in the extreme high-energy limit, when $\phi \to \infty$, the results which we derive would not be affected.) Simplifying approximations such as Eq. (3.19) could not be made in this case. To see this, consider a sequence in which every first-generation pion fathered a second generation, so that $n \propto \phi^2$, and $\ln n \neq \ln\phi$. The number of such sequences (where we require $\phi \gg A$ rather than $\phi \gg 1$) is small compared to the total number of sequences which must be summed over, so we expect the results of numerical calculations for arbitrary ϕ to agree approximately with the results calculated in the limit $\phi \gg A$. We have found this to be the case by explicit numerical calculation.

The result for $(dn/dr)\big|_A^{N_{\max}}$ in Eq. (3.21) is still rather complex, and the investigating of all the regions of experimental and theoretical interest contained therein will occupy the remainder of this section. Let us begin by dividing the numerator and denominator of Eq. (3.21) by σ_1^ϕ in order to set a dimensionless number from which to measure scaling behavior. We find

$$\left.\frac{dn}{dr}\right|_A^{N_{\max}} = \frac{h_1 + \phi S_2(h_1+h_2) + \cdots + \phi^{N_{\max}-1} S_{N_{\max}} \sum_{\alpha=1}^{2^{N_{\max}-2}} b_\alpha \sum_{i=1}^{N_{\max}} c_i^\alpha h_i}{1 + \phi S_2 + \cdots + \phi^{N_{\max}-1} S_{N_{\max}} \sum_{\alpha=1}^{2^{N_{\max}-2}} b_\alpha}, \tag{3.24}$$

where

$$S_N = \frac{\sigma_N^\phi}{\sigma_1^\phi} = \frac{1}{A}\binom{A}{N}\left(\frac{\sigma_{\text{in}}}{\pi R^2 \alpha}\right)^{N-1} \frac{\gamma(N,\alpha)}{\gamma(1,\alpha)}. \tag{3.25}$$

It is obvious that the behavior of the distribution will be governed by the parameter

$$X_N = \phi^{N-1} S_N, \tag{3.26}$$

which depends explicitly on the energy through the power of ϕ, and implicitly on the ϕ dependence of α (recall that in α we allow n to be replaced by ϕ).

As we remarked in Sec. II, the incomplete γ function has two interesting limits, $\alpha \ll 1$ and $\alpha \gg 1$, and interpolates smoothly between them. In discussing high-energy behavior we shall concern ourselves primarily with these limiting forms of the γ function, leaving the intermediate range of α to the numerical calculations.

In these two cases, then, recalling the definition of α, Eq. (2.24),

$$X_N = \begin{cases} \frac{1}{N}\frac{(A-1)!}{(A-N)!}\left(\frac{\phi}{\ln\phi}\frac{1}{A-N}\frac{\sigma_{\text{in}}}{\pi a_{\text{el}}}\right)^{N-1}, & \alpha \gg 1 \quad (3.27a) \\ \frac{1}{N}\frac{(A-1)!}{(A-N)!\,N!}\left(\frac{\phi\sigma_{\text{in}}}{\pi R^2}\right)^{N-1}, & \alpha \ll 1. \quad (3.27b) \end{cases}$$

Since these two forms of X_N appear frequently in the following, it is convenient to define two new parameters,

$$\zeta = \frac{\phi}{\ln\phi}\frac{\sigma_{\text{in}}}{\pi a_{\text{el}}} = \frac{\phi}{\ln\phi}\frac{16}{\pi}\frac{\sigma_{\text{in}}\sigma_{\text{el}}}{\sigma_T^2} \tag{3.28}$$

and

$$\xi = \frac{\phi\sigma_{\text{in}}}{\pi R^2}, \tag{3.29}$$

where we have used the elastic-scattering amplitude of Eq. (2.12) together with the identity

$$\sigma_{\text{el}} = \frac{\pi}{p^2}\int |f_{\text{el}}|^2 dq^2$$

to eliminate a_{el} from the definition of ζ in favor of elementary particle cross sections.

Since we have required from the beginning that $\alpha/(A-N) = (a_{\text{el}}/R^2)\ln\phi$ be small compared to unity [Eq. (2.18)], it is clear that terms in the distribution with $A-N$ small will correspond to $\alpha \ll 1$. If $A-N$ is large, then α may be any size according to the size of $(A-N)(a_{\text{el}}/R^2)\ln\phi$. Setting $N_{\max} = A$, we can study several interesting cases using this type of distinction.

We begin by dividing our systems into "large" or "small," depending on whether $A(a_{\text{el}}/R^2)\ln\phi$ is much greater than or much less than unity. Clearly, this definition is somewhat energy-dependent, but we need not concern ourselves with borderline cases when considering limiting behavior.

For large systems, it is clear that $\alpha \gg 1$ for sequences with small N, and $\alpha \ll 1$ for large N. For terms corresponding to intermediate N, we would simply have to use the incomplete γ function rather than the limiting forms for X_N given in Eq. (3.27). The fact that both $\alpha \gg 1$ and $\alpha \ll 1$ can occur in different terms in the same expression is a major complication in considering large systems. For small systems, however, $\alpha \ll 1$ for all values of N up to $N_{\max} = A$.

Once this basic division is made, we can subdivide further according to different energy regimes

or differentiate between different types of composite systems. In our discussion, we shall concentrate on realistic particle-nucleus collisions, but the same formalism could be used to study scaling in nonrealistic systems which might have theoretical interest, or in hadronic collisions, where the nucleons would be replaced by quarks or partons.

1(a). Large System, Very High Energy

Since ϕ grows logarithmically with the energy, it is obvious that for sufficiently large energy the terms with the highest powers of ϕ will dominate both numerator and denominator in Eq. (3.24). This term corresponds to $N = N_{\max} = A$. This term must dominate not only the terms with $N \approx N_{\max}$ but also those terms with $N \ll N_{\max}$. These requirements are not equivalent in a large system since we have $\alpha \ll 1$ for large N and $\alpha \gg 1$ for small N. However, we can easily calculate the ratio of the $N = A$ term to other terms in the series. We find the ratio of the last term to the next-to-last term to be

$$\frac{X_A}{X_{A-1}} = \frac{\phi\sigma_{\text{in}}}{\pi R^2}\left(\frac{A-1}{A^2}\right) \approx \frac{1}{A}\frac{\phi\sigma_{\text{in}}}{\pi R^2} = \frac{\xi}{A}, \tag{3.30}$$

while we find the ratio of the last term to one of the first few (small-N) terms to be

$$\frac{X_A}{X_N} = \left(\frac{\phi\sigma_{\text{in}}}{\pi R^2}\right)^{A-N}\frac{(A-N)^N}{(N-1)!A}\left(\frac{a_{\text{el}}}{R^2}\ln\phi\right)^N \approx \left(\frac{\phi\sigma_{\text{in}}}{\pi R^2}\right)^{A-N}\left(\frac{a_{\text{el}}}{R^2}\ln\phi\right)^N\frac{1}{(N-1)!}.$$

Obviously, in the limit $\phi \to \infty$, both of these ratios will be large compared to unity, and the $N = A$ term will dominate the expression. If we ask what energy is necessary for this to occur, however, we find that we must have

$$\phi \gg A\,\frac{\pi R^2}{\sigma_{\text{in}}} \tag{3.32a}$$

and

$$\left(\frac{\phi\sigma_{\text{in}}}{\pi R^2}\right)^{A-N} \gg \left(\frac{R^2}{a_{\text{el}}\ln\phi}\right)^N (N-1)! \quad (\text{small } N). \tag{3.32b}$$

For parameters typical of a "large" nuclear system, the satisfaction of the first criterion is sufficient to satisfy the second. If we take $R^2 \approx 5$ fm^2 and $A \approx 10$, we must then have $\phi \gtrsim 100$. The energy associated with a multiplicity this large exceeds the highest known cosmic-ray energies, so the results of this energy regime are of purely theoretical interest. In this limit, we have

$$\frac{dn}{dr} = \frac{\sum_\alpha b_\alpha \sum_i c_i^\alpha h_i}{\sum_\alpha b_\alpha} - O\left(\frac{1}{\xi}\right). \tag{3.33}$$

Since for $\phi \gg A$ $c_1^\alpha = 1$, we have

$$\mathfrak{C}_1 = 1 - O(1/\phi), \tag{3.34a}$$

$$\mathfrak{C}_i = a_i - O(1/\xi), \tag{3.34b}$$

where the a_i are positive numbers of $O(1)$, and from Eq. (3.13)

$$\sum_{i=1}^{A} \mathfrak{C}_i = A - O(A/\xi). \tag{3.35}$$

This case, where $N = A$ dominates, corresponds to a multiplicity so large that every nucleon in the nucleus is likely to undergo an inelastic collision.

1(b). Large System, Low Energy

When ϕ is sufficiently small, the leading term in the denominator will be 1, and in the numerator the leading term for $\mathfrak{C}_i$ will be the first term which contains h_i. This limit will be reached provided that

$$\frac{X_2}{X_N} \approx N\left(\frac{1}{\zeta}\right)^{N-2}, \quad N \ll A \tag{3.36a}$$

and

$$\frac{X_2}{X_A} \approx A\zeta^2\xi^{-A} \tag{3.36b}$$

are both small. Since for real nuclear systems $\zeta \gg \xi$, this limit is reached when $\zeta \ll 1$, i.e., when

$$\frac{\phi}{\ln\phi} \ll \frac{\pi\sigma_T^2}{16\sigma_{\text{in}}\sigma_{\text{el}}}. \tag{3.37}$$

While this would occur at very low energies (a multiplicity of 2–3 for π-N scattering) where our assumption of scaling in the elementary scattering will not hold, it is interesting to note that the criterion is independent of the nucleus. For this case the nuclear coefficients take the form

$$\mathfrak{C}_1 = 1 - O(1/\phi), \tag{3.38a}$$

$$\mathfrak{C}_N = O(\zeta^{N-1}), \quad (\text{small } N), \tag{3.38b}$$

with the remaining $\mathfrak{C}_i$ vanishing still faster.

This case corresponds to a primary collision multiplicity so low that only the primary collision occurs in first approximation.

1(c). Large System, Intermediate Energy

This is the energy region which interpolates the two previously discussed regions, and with the

previous discussion in mind we see that the multiplicity may run from 5 upwards to nearly inaccessible multiplicities. In other words, for large systems this is the region of most interest from the point of view of accelerator or cosmic-ray experiments. At such energies all A terms in the numerator and denominator of dn/dr may contribute to the final answer. We can distinguish between two types of terms—those for which N is small and α is large and those for which N is large and α is small. For the first type of term

$$X_N \approx \frac{1}{N}\zeta^{N-1}, \tag{3.39a}$$

so that the first few terms in numerator and denominator are a power series in ζ. For the second type of term

$$X_N \approx \frac{1}{\Delta!}A^{\Delta-2}\xi^{N-1}, \tag{3.39b}$$

where we have defined

$$\Delta \equiv A - N \ll A . \tag{3.40}$$

The low-energy region is determined by $\zeta < 1$ (and hence small ξ, since for nuclear systems $\xi \ll \zeta$), while the high-energy limit is determined by $\xi \gg 1$. It is then natural to characterize the interpolating region by large ζ but small ξ.

Since there is a single primary collision in every sequence, we still have in this region

$$\mathcal{C}_1 = 1 - O(1/\phi) . \tag{3.41}$$

However, the remaining $\mathcal{C}_i$ are in a state of transition, increasing to their asymptotic values in Eq. (3.34b) in the high-energy limit. Their behavior depends on ζ at the low end of the intermediate-energy region and on ξ at the high end of the intermediate-energy region. In regions of experimental accessibility, for example for energies less than 10 TeV, we would expect that the expression for dn/dr would be dominated by the terms for which Eq. (3.27a) is valid; that is, by terms where X_N is proportional to a power of ζ. Since ζ is independent of the nuclear parameters, we expect that in this intermediate region, which is of most interest experimentally, the nuclear coefficients (and hence the distributions) should be largely independent of the nucleus for "large" nuclei.

2(a). Small System, Very High Energy

The small system is characterized by $A(a_{el}/R^2) \times \ln\phi \ll 1$, so that $\alpha \ll 1$ is appropriate for all X_N. This can be satisfied for some very light nuclei. All X_N are therefore proportional to ξ^{N-1}, and we no longer have to worry about interpolating behavior between ζ and ξ. The very-high-energy limit is reached when X_A terms dominate all others. The criterion is now simply that $(1/A)\xi \gg 1$, or

$$\phi \gg A\,\frac{\pi R^2}{\sigma_{in}} . \tag{3.42}$$

This is the same criterion as for the large system, and the $\mathcal{C}_i$ take forms identical to those of Eq. (3.34). If for a typical small system we take $A \approx 5$, $R^2 \approx 3$ fm^2, then we require $\phi \gtrsim 25$. We may be capable of reaching this limit in cosmic-ray experiments.

2(b). Small System, Low Energy

Remarks and results here are identical to those of 1(b), except we replace ζ by ξ. The criterion that we be in this region is thus $\xi < 1$, or

$$\phi < \frac{\pi R^2}{\sigma_{in}} . \tag{3.43}$$

For realistic systems, this means that ϕ must be less than 4 or so. We are thus not so tightly restricted as for the large system case in our ability to observe this low-energy behavior.

2(c). Small System, Intermediate Energy

As ξ passes through 1 and becomes large we pass through this region. Again, this corresponds to the major experimental range where one might expect IPP-type events to be probable. We have $\mathcal{C}_1 = 1 - O(\phi^{-1})$ again, with the remaining $\mathcal{C}_i$ increasing to their high-energy limits.

C. Limiting Behavior of the Nuclear Distribution

In this part we consolidate the results of Secs. III A and III B to discuss the full nuclear distribution dn/dr. We concentrate on the case of realistic nuclear scattering, so that $\phi \gg \zeta$ or ξ, and in general the distributions h_i reach their limits before their coefficients $\mathcal{C}_i$. For other applications, such as composite models of hadrons, one can easily recompute the distributions; the qualitative form of the high-energy limits will not differ from the nuclear case.

To compute the nuclear scaling behavior for a given regime of energy and A, we look up the relevant forms of the coefficients $\mathcal{C}_i$ defined in Eq. (3.23) and discussed in Sec. III B, and combine them with the forms of the h_i from Sec. III A, using the relation (3.23).

Table I shows the analytic behavior of the nuclear distribution according to the categories in Sec. III B and according to the fragmentation and pionization regions. In Sec. IV we illustrate this behavior with some numerical examples.

TABLE I. The asymptotic form of the single-particle distribution together with the nonasymptotic corrections as a function of the type of composite target and the energy of the projectile.

	Nuclear distribution dn/dx				How is limit approached?		
	Target fragmentation			Projectile fragmentation	Target fragmentation	Pionization	Projectile fragmentation
	$-1<x<-A^{-1}$	$-A^{-1}<x<-x_W$	Pionization	$x_W<x<1$			
Large system, very high energy $A\gtrsim 10$, $\phi\gtrsim 100$; $\xi, \xi\gg A$	0	$Ah_1(Ax)$	definite limit	$h_1(x)$	from below, as A/ξ	from below	from below, as $1/\phi$
Large system, intermediate energy $A\gtrsim 10$, $\phi\approx 2-100$; $\xi\gg 1$, $\xi\ll 1$	0	interpolates low and high energy		$h_1(x)$	increasing, rate governed by ξ for smaller ϕ, by ξ for larger ϕ	increasing, rate governed	from below, as $1/\phi$
Large system, low energy $A\gtrsim 10$, $\phi\lesssim 2$; $\xi, \xi\lesssim 1$	0	$h_1(Ax)-O(1/\phi)+O(A\xi)$	$h_1(x)-O(1/\phi)+O(\xi)$	$h_1(x)$	no limit, just approximate scaling		
Small system, very high energy $A\lesssim 5$, $\phi\gtrsim 25$; $\xi\gg A$	0	$Ah_1(Ax)$	definite limit	$h_1(x)$	from below, as A/ξ	from below	from below, as $1/\phi$
Small system, intermediate energy $A\lesssim 5$, $\phi\approx 4-25$; intermediate ξ	0	interpolates low and high energy		$h_1(x)$	increasing, rate governed by ξ	increasing, rate governed	from below, as $1/\phi$
Small system, low energy $A\lesssim 5$, $\phi\lesssim 4$; $\xi\lesssim 1$	0	$h_1(Ax)-O(1/\phi)+O(A\xi)$	$h_1(x)-O(1/\phi)+O(\xi)$	$h_1(x)$	no limit, just approximate scaling		

We make the following explicit comments about the table and our general results.

(i) In the target-fragmentation region there is no distribution for $x<-A^{-1}$, and the scaling function is $h_1(Ax)$ rather than $h_1(x)$. This is simply because x is approximately the fractional target momentum in the center-of-mass system. Since at high energies the A constituents of the target are weakly bound, each constituent carries A^{-1} of the target momentum, and therefore no pion can be detected in the backward hemisphere with more than A^{-1} of the target momentum. Similarly, while the input target distribution function has argument x in the projectile-nucleon system, in the projectile-nucleus system this pion-nucleon distribution function must have argument Ax.

(ii) In the projectile-fragmentation region, the nuclear distribution approaches the pion-nucleon distribution function h_1 in its projectile-fragmentation region. This follows from the fact that in this region all the h_i approach zero as ϕ^{-1} except h_1 itself, regardless of the behavior of their coefficients $\mathfrak{C}_i$, while $\mathfrak{C}_1=1-O(\phi^{-1})$. In the target-fragmentation region, the nuclear distribution approaches a limiting value which is A times the elementary distribution. This follows from the general result [see Eq. (3.4a)] that in this region all h_i approach h_1 as ϕ^{-1}, and that

$$\sum_{i=1}^{A}\mathfrak{C}_i=A-O\left(\frac{A}{\xi}\right)$$

[see Eq. (3.35)].

Note that the approach to scaling in the target-fragmentation region is governed by ϕ, while in the projectile-fragmentation region it is governed by ξ. Thus the approach to scaling is faster in the projectile region than in the target region.

(iii) Our results illustrate two forms of independence of fragmentation regions. The first and stronger (in the sense that fewer assumptions are required) form is that, given the pion-nucleon distribution in the pion-fragmentation region, this distribution remains asymptotically unchanged when we scatter pions from a target composed of any number of nucleons. (We shall speculate along these lines in Sec. V.) The second and weaker form states that if we start with a pion-hadron distribution with independent fragmentation regions, then our composite-system scattering distributions certainly retain this property.

(iv) The linear behavior in A of our limiting results may at first appear surprising, because we have grown used to thinking in terms of surface ($\sim A^{2/3}$) effects in high-energy hadron-nucleus scattering. This result follows from the fact that we are computing a number distribution, and not a cross section. To convert our results to a cross

section, it is necessary to multiply dn/dr by the normalization factor σ_{in}^{T} [see Eq. (2.10)]. This factor, which is the inelastic pion-nucleus cross section, contains the hadronic A dependence, and is usually said to behave according to an "$A^{2/3}$" law.

We also note that in our calculation there is no mechanism by which a pion can be absorbed in the nucleus. The pion either emerges after scattering elastically, or it scatters inelastically, creating other pions. [In extremely large systems (such as neutron stars) this would not be the case, and our results could not be expected to apply.] Note that while factors like $1-\Gamma_{\text{el}}$ are normally thought to give absorption, we are here taking *explicit* account of the allowed inelastic channels in which this absorption will take place. All these inelastic channels lead to pions in the final state.

IV. NUMERICAL EXAMPLE

In this section we present the results of computer calculations of the nuclear distribution. This can include computations of the h_i, summation over sequences, and calculation of the σ_N^n using Eq. (2.11). We simplify this procedure in two ways. Firstly, we use as a $\pi+N\to\pi+X$ input distribution h_1 a step function of height 1 from $x=-1$ to $x=+1$. As we previously discussed, for such a function we can compute the h_i analytically, as in Eq. (3.6). Secondly, the form for σ_N^n in Eq. (2.11) is not directly susceptible to numerical integration for large values of ϕ. This is because of the second sum in brackets in that equation, which involves the summation of high-order binomial coefficients with alternating sign. The resulting very large cancellations cause difficulty. As we discussed in Eq. (2.15) ff., this can be circumvented by expanding in the small parameter a_{el}/R^2, with coefficients S_m, as in the Appendix. We use this procedure, keeping both S_1 and S_2 (i.e., up to $O((a_{\text{el}}/R^2)^2)$, given by Eqs. (A7) and (A11), in order to perform the numerical integration over y.

Additionally, time limitations did not allow us to take $N_{\max}=A$ for any A. However, the qualitative behavior of the high-energy limits in Table I is reproduced for *any* fixed $N_{\max}$. The only quantitative change is that the factor A multiplying $h_1(Ax)$ in the target-fragmentation column becomes a factor $N_{\max}$. Therefore we are still able to make meaningful numerical computations.

The process we have chosen is $\pi+{}^9\text{Be}\to\pi+X$. In this nucleus the root mean square radius is 2.2 F. We can take for pion-nucleon parameters $a_{\text{in}}=a_{\text{el}}=10\ \text{GeV}^{-2}$ and $\sigma_{\text{in}}=4$ mb. In addition, we run ϕ up from 5 to 25. If we take a typical value of n, then $\ln n$ will be ~3. This gives us

$$\frac{a_{\text{el}}\ln n}{R^2}\approx 0.3\,.$$

We computed up to $N_{\max}=6$. In this range

$$(A-N_{\max})\frac{a_{\text{el}}\ln n}{R^2}=O(1)\,,$$

the nucleus is a "large" system, and we are just beginning to make the transition from ζ-type to ξ-type behavior. Therefore in most of the range we discuss ζ-type behavior is dominant. This became numerically apparent when we repeated our calculations for larger nuclei and found the results to differ from the ^{9}Be results we are about to present by only a few percent.

We begin with a calculation in the low-energy regime of Table I. By taking the pion-nucleon parameters as above, except $\sigma_{\text{in}}=2$ rather than 4 mb, we find $\zeta<1$ over the entire range of ϕ rather than $\zeta>1$ over much of the ϕ range. This is just the situation corresponding to low energy. Figure 2 shows the nuclear distribution plotted as a function of x. $N_{\max}$ has been fixed at 5, although these results are quite insensitive to $N_{\max}$. We see the linearly increasing ϕ behavior near unity in the target-fragmentation region, as well as the stability of the projectile-fragmentation region near unity.

Next we return to the case $\sigma_{\text{in}}=4$ and fix $N_{\max}=6$. As we increase ϕ the target-fragmentation region distribution should approach the limit 6 for $-\frac{1}{9}<x<0$, and, in smaller steps, the projectile-fragmentation region distribution should approach the limit unity for $0<x<1$. In the pionization region, the distribution should approach an intermediate limit. Figure 3 shows the distribution as a function of x to illustrate the fragmentation regions, and Fig. 4 shows the distribution as a function of center-of-mass rapidity to illustrate the pionization region. The qualitative behavior we have discussed appears in a rather striking fashion. To probe this distribution a bit more deeply, Fig. 5 shows the behavior of the coefficients $\mathcal{C}_i$ of the distributions h_i, as we discussed in Eq. (3.34) and Sec. III B 1(c). We see $\mathcal{C}_1$ fairly quickly approaching the value unity, and the remaining $\mathcal{C}_i$ approaching definite limits less quickly. Their sum also approaches a limit near to 6.

The authors are preparing a paper which will contain results of calculations for realistic nuclei and realistic elementary distributions, and the interested reader is referred to that work for further numerical studies.

V. DISCUSSION

Having presented the main results in the previous two sections, we devote this section to two

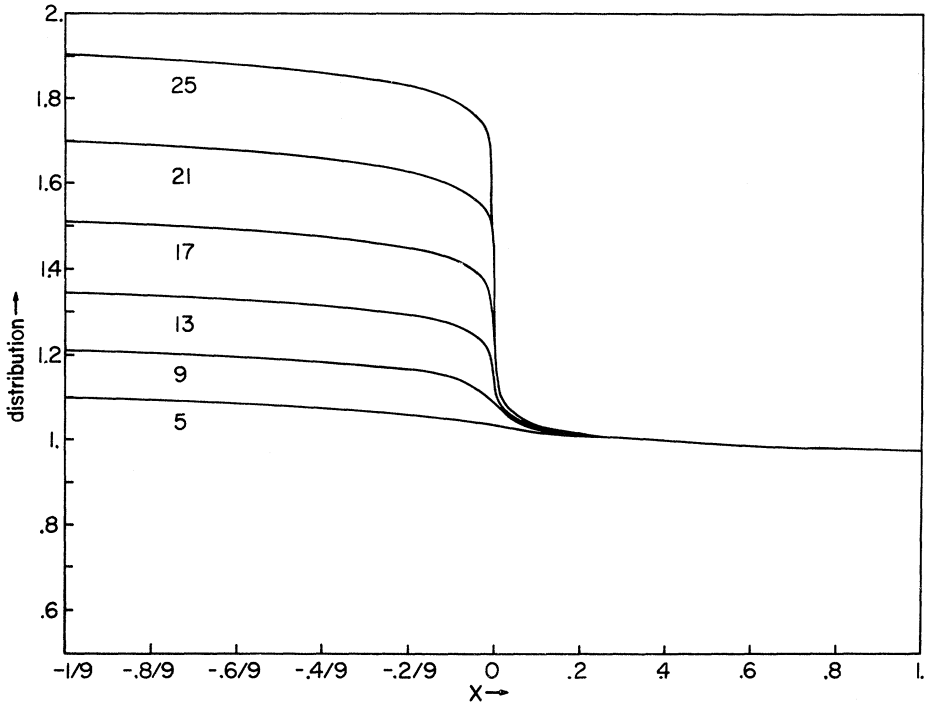

FIG. 2. Distribution of pions in $\pi + A \rightarrow \pi + X$. The input pion-nucleon distribution is everywhere equal to unity. $N_{max} = 6$, and the parameters are chosen (see text) such that the indicated range of ϕ is a "low-energy" range. Note the uniform nonscaling departure from the input distribution.

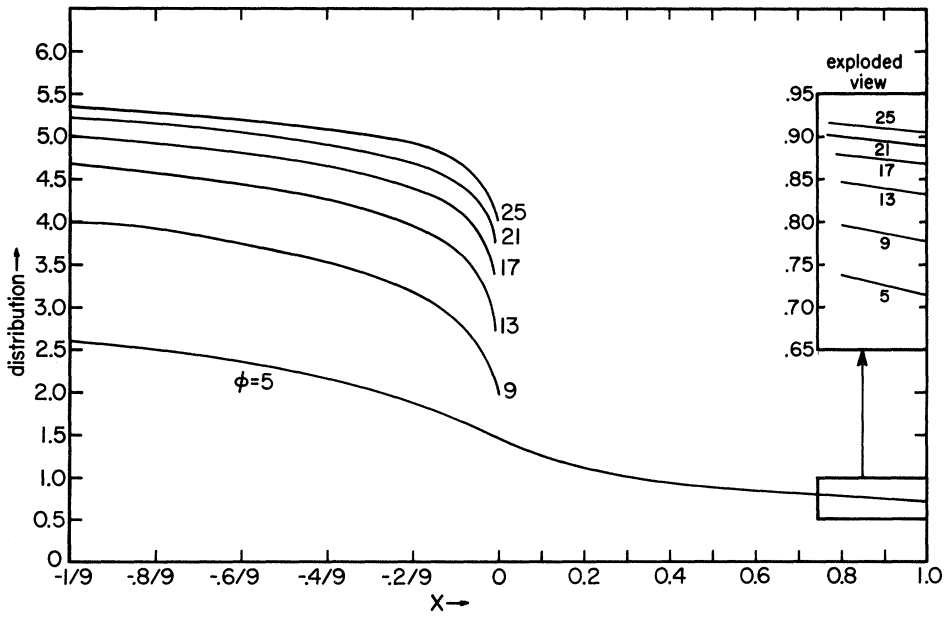

FIG. 3. Distribution of pions in $\pi + A \rightarrow \pi + X$ plotted as a function of longitudinal momentum fraction x. $N_{max} = 6$, and the parameters are realistic ones (see text) such that the indicated range of ϕ is an "intermediate to high-energy" range. Note the approach to a scaling distribution.

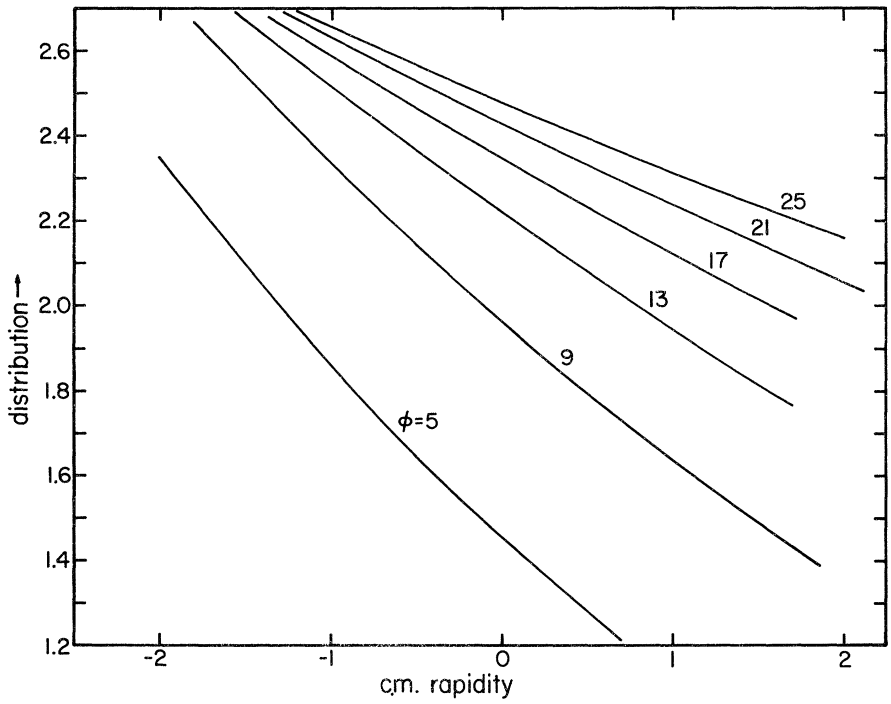

FIG. 4. As in Fig. 3, but distribution plotted as a function of center-of-mass rapidity to show central region.

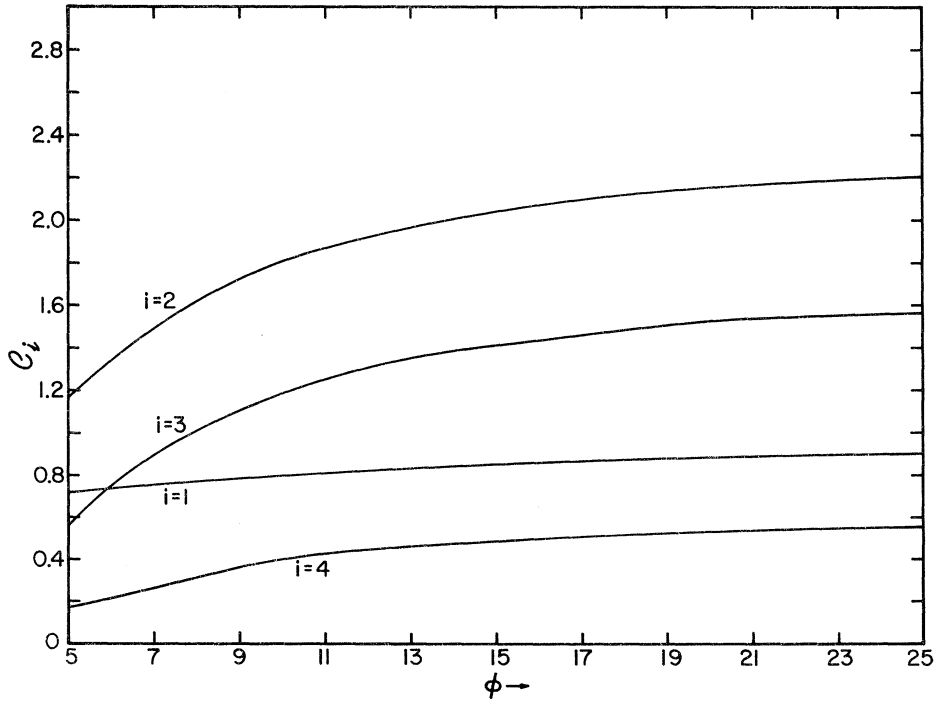

FIG. 5. Behavior of the distribution coefficients c_i as a function of ϕ. Note the rise to asymptotic values.

main topics. First, we discuss the possible tests and applications of our ideas to accelerator and cosmic-ray experiments on nuclear targets. Second, we discuss and speculate on the role our ideas may play in understanding the hadrons themselves, pointing out new ways to look at some characteristics of hadronic properties as well as the possible connections of our ideas with other approaches to these characteristics.

A. Experimental Tests

The original and still valid motivation to study cascading in nuclei, which we first discussed in Ref. 7, was to help distinguish between incoherent production processes (IPP) such as multiperipheralism and coherent production processes (CPP) such as diffractive excitation. Because, e.g., a diffractive excitation lives for a very long time compared to nuclear radii at high energies, CPP models do not cascade as we have discussed above, although the excitation itself may rescatter. On the other hand, IPP models can give cascading as we have discussed it. Thus a simple way to distinguish between IPP and CPP models is to measure the multiplicity of pions in nuclear collisions. An increasing excess over πP multiplicity in this quantity would favor IPP models. We shall discuss these distinctions in more detail elsewhere.

Assume that IPP behavior dominates at some accessible value of energy. By appropriate choice of nucleus the actual distributions we discuss above can then be tested. Available ϕ runs roughly from 5 to 25, the latter in $\gtrsim 10^4$-GeV cosmic rays. We can then test the behavior in α by an appropriate choice of nucleus, and should see either an approach toward a limit or a transition region from ζ- to ξ-type behavior. In particular it should be possible to verify that the projectile-fragmentation-region number distribution is unaffected by the choice of nucleus.

There are many aspects of our problem that deserve further theoretical attention from this practical point of view. First, a mixture of IPP and CPP (which at present appears to be a satisfactory way to explain hadronic data[14]) should be treated. Nuclear scattering remains a very attractive method to help pin this mixture down more closely. Second, we have integrated over the transverse momentum. It would be interesting to see if a richer structure emerges when we do not do so. As a guess, we recall that the transverse momentum structure in the incoherent production of exclusive channels is the same on nuclei as on hadron targets. Perhaps this result is also true for the inclusive distributions. Third, we have treated number distribution in only an average way; our results assume (and result in) no dispersion in the number of outgoing pions. Such effects could be treated by Monte Carlo methods. This is important as it relates to two-particle (and higher) inclusive measurements. Such measurements are presently our principal tools for distinguishing IPP and CPP behavior in hadronic collisions. It would be most interesting to study such quantities in hadron-nucleus collisions.

In summary, the study and possible behavior of hadron-nucleus inclusive distributions presents us with a very rich field of exploration. Such exploration can shed useful light on the nature of hadronic interactions.

B. Speculations on Hadronic Reactions

If we want to try to apply these ideas and methods to hadronic processes by assuming that hadrons are composite systems whose constituents are partons, then the complexity of the phenomena we have discussed provides us with many possibilities to choose from. Is hadronic scattering in a region of approximate scaling at AGS or NAL energies, as in the low-energy regions of Table I? Or is hadronic scaling at a true scaling limit, as in the high-energy regions? Regardless of these distinctions, there are some systematic features necessary in such a treatment, which we discuss below.

Unlike the nucleus, which has a fixed number of constituents, we might expect the hadronic state to be a superposition of states with differing numbers of partons. During the brief time of an hadronic collision, we have a certain probability of being in an n-parton state. We expect the kind of multiple scattering we have discussed to occur when the n partons are weakly bound, in the sense that the partons carry fixed fractions of the momentum. The longitudinal cutoff in x occurs for the n-parton state at $1/n$. In addition, the limiting distributions are approached from below. Combining these facts, there are then three conclusions to be made.

(i) If we want our distribution to reach to $x=1$, then the one-parton state is important. (Note that this "one-parton state" may be a *strongly* bound system in itself.) As we move x down from 1, states with higher numbers of partons begin to contribute, *increasing* the distribution. We therefore expect a distribution smoothly increasing as $|x|$ runs from 1 to 0—recall that each parton-parton reaction must also be of the IPP type for this result to hold.

(ii) Recall from Table I that the approach to a limiting distribution for an n-parton system depends linearly on n. Therefore we expect the scal-

ing limit to be approached more slowly at smaller values of $|x|$.

(iii) As in nuclear scattering, we would expect to approach limiting behavior from below. Combined with (ii) above, we expect the distribution to increase in general, and to increase most rapidly in the small-$|x|$ region, until the limiting behavior is reached.

Remarkably enough, except for "leading particle" peaks in the inclusive distribution, which would appear to be due to a kind of diffractive excitation, these qualitative results seem to be true. Particularly with regard to (iii), note that this approach to scaling follows without the recourse to the lower-lying trajectories one requires in a Mueller-type analysis.[15] Mueller analysis also states that the rate of approach goes like s^p, where $p \approx \frac{1}{4}$. On the other hand, the rate of approach we find depends approximately linearly on the multiplicity, i.e., logarithmically on s. We do not know whether logarithmic energy dependence would fit the observed approach to scaling.

The picture we present is a recursive picture of several aspects of dynamical behavior. In the first place, the simplest such aspect is scaling itself. If the scattering of the constituents scales, then so too does the scattering of the composite system. In the second place, we can understand the independence of fragmentation regions in a recursive way. Imagine that all hadronic systems are made of the same kind of partons. Then the stronger form of fragmentation-region independence we discussed in Sec. IIIC automatically implies that hadronic scattering will exhibit this independence feature. If on the other hand all nucleons were not made of the same kind of partons, then we would require the weaker form of fragmentation-region independence for the parton-parton amplitude to imply independence for hadronic scattering. In the third place, we can qualitatively see that particle-number dispersion will be affected by multiple scattering. With a given number distribution in the parton-parton collision itself, there will be a further effect on the number distribution due alone to energy differences in the particles producing the collisions of second and higher generation. It would then be most interesting to see if it would be possible to have the output number distribution in hadron-hadron collisions equal to the input number distribution in the parton-parton collision. This would constitute a recursive understanding of this number distribution, and therefore of the model for hadronic reactions for which this distribution applies.

One rather nice logical consequence of extending this kind of thinking to its extreme is that it introduces a kind of self-consistency into the picture in which matter is considered to be made up of layers. If we hypothesize a requirement such as scaling at some level (for example, in the interactions of partons), then it also appears in other levels (for example, in the interactions of elementary particles).

APPENDIX

We consider a sum relevant to the nuclear weight factors,

$$S_m = \sum_1^{2n} \binom{2n}{k} \frac{(-x)^k}{k^m} . \tag{A1}$$

Note that the summation index starts with 1 rather than 0. To treat this sum, start with S_1 and differentiate with respect to x. The resulting sum is just a binomial series,

$$\frac{d}{dx} S_1 = \frac{1}{x}[(1-x)^{2n} - 1],$$

or

$$S_1 = \int_0^x dx \, \frac{(1-x)^{2n} - 1}{x} . \tag{A2}$$

By making the transformation $y = 1 - x$, the integrand becomes $\sum_{m=0}^{2n-1} y^m$, which we may integrate over y from 1 to $1 - x$ term by term. Thus

$$S_1 = \sum_1^{2n} \frac{(1-x)^k - 1}{k} . \tag{A3}$$

We can now proceed by induction, noting that

$$\frac{d}{dx} S_m = + \frac{1}{x} S_{m-1},$$

or

$$S_m = \int_0^x dx \, \frac{1}{x} S_{m-1} . \tag{A4}$$

The same transformation $y = 1 - x$ of the integrand shows us that

$$S_m = \sum_{l_1=1}^{2n} \frac{1}{l_1} \sum_{l_2=1}^{l_1} \frac{1}{l_2} \cdots \sum_{l_m=1}^{l_{m-1}} \frac{(1-x)^{l_m} - 1}{l_m} \tag{A5}$$

is a solution to the recursion relation of Eq. (A4).

Application of these series in our case occurs for x between 0 and 1. A simple test for their convergence as $n \to \infty$ is Ermakov's rule, which implies divergence. This is easy to see by noting that at large n the 1 term in the numerator is dominant over the $(1-x)^{l_m}$ term. Estimation of the sum by integral approximation for large n then gives

$$S_m \approx -\int^{2n} \frac{dz_1}{z_1} \int^{z_1} \frac{dz_2}{z_2} \cdots \int^{z_{m-1}} \frac{dz_m}{z_m}$$
$$\approx -\frac{1}{m!}(\ln 2n)^m$$
$$\approx -\frac{1}{m!}(\ln n)^m . \quad \text{(A6)}$$

For use in our numerical computations we want to be a bit more precise and keep up to constant terms in S_1 and S_2, because for large n the multiple sums are expensive to compute directly. The two terms in S_1 are well known individually, so that ignoring terms of $O(1/n)$

$$-S_1 \cdot + \ln 2n + \ln x + C , \quad \text{(A7)}$$

where $C \simeq -0.5772$ is Euler's constant. By making the substitution $y = 1 - x$, we can also split up S_2:

$$S_2 = \sum_{k=1}^{2n} \frac{1}{k} \sum_{l=1}^{k} \frac{y^l}{l} - \sum_{1}^{2n} \frac{1}{k} \sum_{1}^{k} \frac{1}{l}$$
$$= \sum_{k=1}^{2n} \frac{1}{k} \sum_{l=0}^{k-1} \int_0^y dz\, z^l - \sum_{1}^{2n} \frac{1}{k} \sum_{1}^{k} \frac{1}{l} . \quad \text{(A8)}$$

It is simple to show that the first sum is given by

$$-\tfrac{1}{2}\ln^2 x - \ln x \ln 2n - C \ln x + O((1-x)^{2n} \ln^2 x) . \quad \text{(A9)}$$

We estimate the second sum by means of the Euler-MacLaurin method. The series has $\ln^2 n$, $\ln n$, and constant terms. The x-independent constant terms consist of various complicated sums over Bernoulli numbers B_l and ζ functions which we combine and eventually determine numerically. Additionally, one of the $\ln n$ terms has a coefficient

$$\sum_{l=1}^{\infty} \frac{B_{2l}}{2l} ,$$

which we recognize as $C - 0.5$. Otherwise the evaluation is straightforward. We find for this second sum the result

$$\tfrac{1}{2}\ln^2 2n + \tfrac{1}{2}\ln 2n + (C - 0.5)\ln 2n - 0.99128 . \quad \text{(A10)}$$

By combining the expressions in (A9) and (A10) we find

$$-S_2 \approx \tfrac{1}{2}\ln^2 2n + (C + \ln x)\ln 2n + C \ln x + \tfrac{1}{2}\ln^2 x - 0.99128 . \quad \text{(A11)}$$

---

*Work supported in part by the Center for Advanced Studies, University of Virginia, and in part by the National Science Foundation under Grant No. GP-32998X.

†Permanent address.

[1]J. Benecke, T. T. Chou, C. N. Yang, and E. Yen, Phys. Rev. **188,** 2159 (1969).
[2]R. P. Feynman, Phys. Rev. Lett. **23,** 1415 (1969).
[3]R. P. Feynman (unpublished); J. D. Bjorken and E. A. Paschos, Phys. Rev. **185,** 1975 (1969).
[4]P. M. Fishbane and J. S. Trefil (unpublished).
[5]D. Amati. S. Fubini, and A. Stanghellini, Nuovo Cimento **26,** 896 (1962).
[6]R. C. Hwa, Phys. Rev. Lett. **26,** 1143 (1971); M. Jacob and R. Slansky, Phys. Rev. D **5,** 1847 (1972).
[7]P. M. Fishbane and J. S. Trefil, Phys. Rev. D **3,** 238 (1971).
[8]P. M. Fishbane, J. L. Newmeyer, and J. S. Trefil, Phys. Rev. Lett. **29,** 685 (1972); P. M. Fishbane, J. S. Trefil, and J. L. Newmeyer, Phys. Rev. D 7, 3324 (1973).
[9]R. J. Glauber, in *High Energy Physics and Nuclear Structure,* edited by G. Alexander (North-Holland, Amsterdam, 1967), pp. 311 ff.
[10]P. M. Fishbane, J. L. Newmeyer, and J. S. Trefil, Phys. Lett. **41B,** 153 (1972).
[11]See also A. Dar and J. Vary, Phys. Rev. D **6,** 2412 (1972).
[12]This provides an "absorption" factor in more usual applications. See J. S. Trefil and F. von Hippel, Phys. Rev. D **7,** 2000 (1973); see also Ref. 8.
[13]J. S. Trefil, Phys. Rev. D **3,** 1615 (1971); Nucl. Phys. **B29,** 575 (1971); Trefil and von Hippel, Ref. 12.
[14]C. Quigg and J. D. Jackson, NAL Report No. NAL-THY-93 (unpublished).
[15]A. H. Mueller, Phys. Rev. D **2,** 2963 (1970).